Atomic Force Microscopy Study of Helical Poly(phenylacetylene)s on a Mica Substrate

Shin-ichiro Sakurai,[†] Kenji Kuroyanagi,[†] Kazuhide Morino,[†] Masashi Kunitake,[‡] and Eiji Yashima*,[†]

Department of Molecular Design and Engineering, Graduate School of Engineering, Nagoya University, Chikusa-ku, Nagoya 464-8603, Japan, and Department of Applied Chemistry & Biochemistry, Faculty of Engineering, Kumamoto University, Kumamoto 860-8555, Japan

Received September 2, 2003
Revised Manuscript Received October 2, 2003

The study of the structure and morphology of biological[1] and synthetic[2−4] polymers on a solid surface using atomic force microscopy (AFM) has aroused considerable interest in recent years and has been extended to the design and construction of novel nanostructured materials.[5] Single chains of synthetic macromolecules, for instance, homopolymers, block polymers, and graft polymers,[2] hyperbranched polymers,[3] and polyelectrolytes,[4] have been visualized and examined by AFM regarding their structures and conformations. However, very few attempts have been made to observe synthetic helical polymers using AFM[6] and scanning tunneling microscopy (STM).[7]

We previously reported that optically inactive, stereoregular poly(phenylacetylene)s bearing various functional groups can form a one-handed helix and exhibit an induced circular dichroism (ICD) in the UV−visible region of the polymer backbone spectrum upon complexation with chiral molecules interacting with the polymer's functional groups in organic solvents[8] as well as in water.[9] The changes in conformation of the poly(phenylacetylene)s with or without chiral small molecules in solution have been studied by means of CD and ^{1}H NMR spectroscopies.[8,9] In this study, we report the AFM studies of poly((4-carboxyphenyl)-acetylene)s with low (poly-**1L**) and high molecular weights (poly-**1H**) and their complexes with (*R*)-(+)-1-(1-naphthyl)ethylamine ((*R*)-Nap) on solid substrates. Single molecules of these polymers can be directly visualized, and changes in the conformation and morphology of poly-**1** upon complexation with (*R*)-Nap, resulting in an induced helical structure, were examined on a mica surface using AFM. An optically active poly(phenylacetylene) having an (*R*)-Nap residue covalently bonded as the pendant, poly((*R*)-(−)-(4-((1-(1-naphthyl)ethyl)carbamoyl)phenyl)acetylene) (poly-(*R*)-**2**), was also prepared as the model polymer,[10] and its structure was also investigated by AFM for comparison.

Figure 1 shows the structures of poly-**1**, poly-(*R*)-**2**, and (*R*)-Nap and the calculated helical conformation of poly-(*R*)-**2** (20-mer) together with a helical poly-**1** model (20-mer) for comparison. The *cis*−*transoidal* stereoregular poly-**1L** and poly-**1H** were prepared according to a previously reported method using a water-soluble rhodium complex in water.[9b] The number average molecular weights and polydispersities of poly-**1L** and poly-**1H** were $M_n = 3.3 \times 10^4$ and $M_w/M_n = 2.8$ and $M_n = 1.3 \times 10^5$ and $M_w/M_n = 4.3$, respectively. Poly-(*R*)-**2** bearing the chiral (*R*)-Nap group connected to the poly(phenylacetylene) backbone via an amide bond was also prepared in the same way ($M_n = 3.0 \times 10^5$ and $M_w/M_n = 1.8$).[10c]

AFM analyses of poly-**1L** and poly-**1H** with and without (*R*)-Nap on a freshly cleaved mica surface or a highly oriented pyrolytic graphite (HOPG) were conducted to observe changes in the morphology and conformation of the polymer main chains. Figure 2 shows typical AFM images of poly-**1L** and poly-**1H** with and without (*R*)-Nap on mica. Under a relatively high poly-**1H** concentration (0.5 mg/mL), the mica substrates were covered with a nanostructured network and wormlike poly-**1H** chains (Figure 2A), while individual poly-**1H** chains complexed with (*R*)-Nap can be visualized on mica (Figure 2B).[11] The average height of the poly-**1H**−(*R*)-Nap complex in Figure 2B was estimated to be 0.87 ± 0.25 nm, which was shorter than that of the networked poly-**1H** (1.22 ± 0.23 nm) observed in Figure 2A. The difference in the height of the poly-**1H** and the poly-**1H**−(*R*)-Nap indicates that poly-**1H** deposited from a highly concentrated solution on mica forms an interchained polymer network, probably through hydrogen bonding of the intermolecular carboxy groups of the polymer, and such an intermolecular network could be released upon complexation with (*R*)-Nap.

Stretched single molecules of poly-**1H** and the poly-**1H**−(*R*)-Nap complex can be directly visualized on mica prepared from a dilute solution of poly-**1H** (0.05 mg/mL) (Figure 2C and D). We note that the poly-**1H** and poly-**1L** complexed with (*R*)-Nap showed a full ICD under the dilute concentrations in a 0.34 M DMSO solution of (*R*)-Nap. The average height of the separately adsorbed poly-**1H** molecules was determined to be 0.67 ± 0.10 nm from ∼100 cross section profiles in Figure 2C, which increased to 0.83 ± 0.15 nm after complexation with (*R*)-Nap (Figure 2D). These values were shorter than the computer-generated molecular diameters of a helical poly-**1** (1.5 nm) and poly-**1H**−(*R*)-Nap complex (2 nm). The strong interaction of the polymer with the mica surface and the decompression of the polymer due to solvent vaporization as well as a tip-induced deformation of the samples should be taken into consideration for the reduced heights of poly-**1H** and the poly-**1H**−(*R*)-Nap complex on mica.[12]

AFM images of poly-**1L** with and without (*R*)-Nap are shown in Figure 2E and F. As observed for poly-**1H** and the poly-**1H**−(*R*)-Nap complex, single molecules with stretched chains of poly-**1L** and poly-**1L** complexed with (*R*)-Nap were observed prepared from a diluted solution (0.05 mg/mL). The average height of poly-**1L** (0.60 ± 0.15 nm) increased through the helix formation induced by (*R*)-Nap (0.78 ± 0.14 nm). In the AFM analysis, the vertical resolution of the AFM images is much better than the horizontal resolution because of overestimation due to the broadening effect of the

* To whom correspondence should be addressed. E-mail: yashima@apchem.nagoya-u.ac.jp.
[†] Nagoya University.
[‡] Kumamoto University.

10.1021/ma035290t CCC: $25.00
Published on Web 11/11/2003

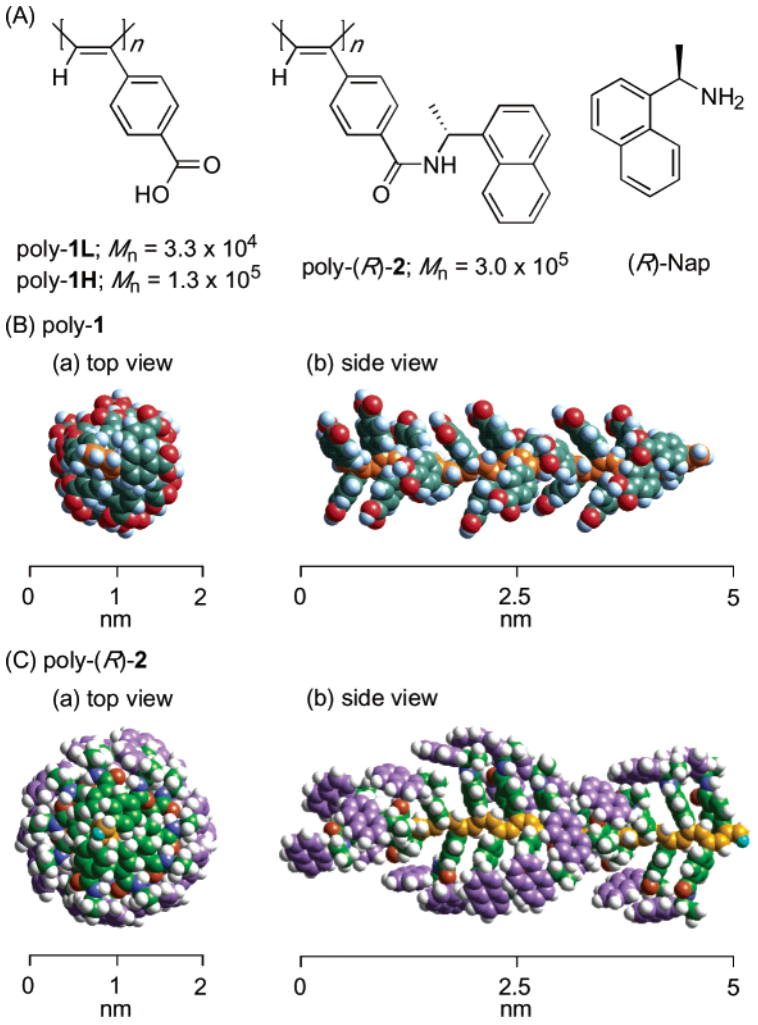

Figure 1. Structures of poly-**1**, poly-(*R*)-**2**, and (*R*)-Nap (A) and possible right-handed helical structures of poly-**1** (B) and poly-(*R*)-**2** (20-mer) (C). The helix-sense of poly-(*R*)-**2** is tentative, but the polymer should have a helical conformation, as it exhibits an ICD in the main chain region.

tip.[13] To exclude the difference in the broadening effect of the tips, we measured the AFM images of poly-**1L** and the poly-**1L**−(*R*)-Nap complex using the same tip under the same conditions and then obtained almost the same results, so that it is concluded that the difference in the height observed for both the polymers is a valuable fact.

To further investigate in detail the differences in the average heights between the poly-**1L** and poly-**1H** and their complexes with (*R*)-Nap, the structure and conformation of poly-(*R*)-**2**, a model polymer of the poly-**1**−(*R*)-Nap complex on mica, were investigated with AFM. Figure 3 shows the AFM images of poly-(*R*)-**2** deposited on mica from a DMF solution (0.025 mg/mL).[14] The average height of single stranded poly-(*R*)-**2** was estimated to be 0.88 ± 0.14 nm from ∼100 cross section profiles. This height value was close to those of the poly-**1L** and poly-**1H** complexed with (*R*)-Nap (poly-**1L**, 0.78 ± 0.14 nm; poly-**1H**, 0.83 ± 0.15 nm). These results indicate that the increased height of the poly-**1** molecules complexed with (*R*)-Nap on the mica surface is ascribed to the complexation with (*R*)-Nap through an acid−base interaction, and this complexation results in the one-handed helical structure, which can be detected by AFM.[15]

The more detailed observation of the AFM images in Figures 2 and 3 gave us useful information regarding the structures of the polymers. The height and phase images of the poly-**1H**−(*R*)-Nap complex (Figure 4A and B), which were obtained by expanding the images in Figures 2D and 3, respectively, feature a particularly interesting conformation and supramolecular structure of the complex. An extended single strand of the poly-**1H**−(*R*)-Nap complex can be visualized on mica (a). Double strands of the poly-**1H**−(*R*)-Nap complex with a 1.54 nm height agglomerate to form the toroidal structure (b). A single chain of the poly-**1H**−(*R*)-Nap complex marked by (c) in Figure 4B seems to adopt a left-handed helical structure. Such a helical shape image may be closely correlated to the macromolecular helical chirality of the poly(phenylacetylene)s. In Figure 4D, a helically twisted, single stranded, right-handed helical structure was observed for poly-(*R*)-**2** in part on mica in the phase image by taking into consideration the height (Figure 4C, 0.83 nm). The helix-sense observed for poly-(*R*)-**2** (right-handed) is opposite that observed for the poly-**1H**−(*R*)-Nap complex (left-handed), which is consistent with the CD data of the polymers; the second Cotton CD intensity ($[\theta] \times 10^{-4}$ deg cm^2 dmol^{-1}) is −3.08 (poly-**1H**−(*R*)-Nap) and +2.74 (poly-(*R*)-**2**) in DMSO and DMF, respectively.[10c]

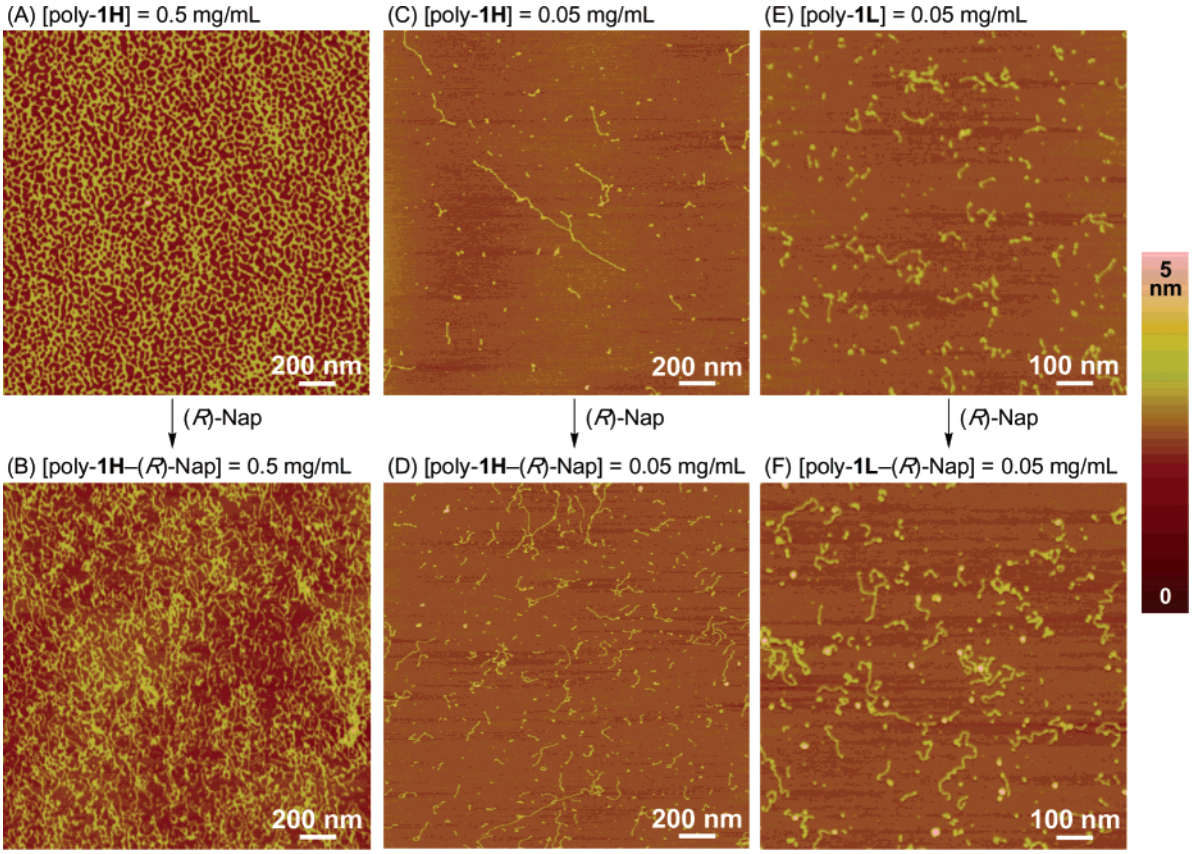

Figure 2. AFM tapping mode images of poly-**1H** (A and C), the poly-**1H**−(*R*)-Nap complex (B and D), poly-**1L** (E), and the poly-**1L**−(*R*)-Nap complex (F) on mica. The concentrations of poly-**1H** are 0.5 (A and B) and 0.05 mg/mL (C and D) in DMSO (A and C) and a 0.34 M DMSO solution of (*R*)-Nap (B and D). The concentration of poly-**1L** is 0.05 mg/mL (E and F) in DMSO (E) and a 0.34 M DMSO solution of (*R*)-Nap (F).

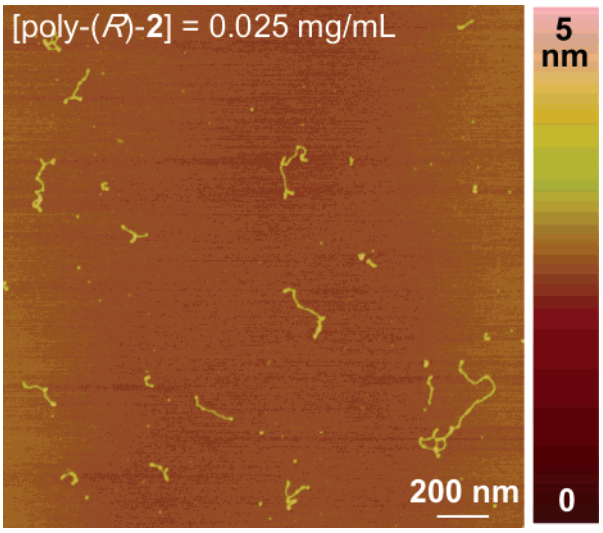

Figure 3. AFM tapping mode image of poly-(*R*)-**2** on mica. The concentration of poly-(*R*)-**2** is 0.025 mg/mL in DMF.

These experimental results demonstrate that a helical conformation induced on the poly-**1** backbones in the presence of the (*R*)-Nap and poly-(*R*)-**2** could be observed directly using AFM, although the assignments of the CD bands with respect to the polymer conformations cannot be completely understood. Apparently, a further study using STM may be necessary to detect the atomic level conformation of these polymers.[7]

In conclusion, the present studies showed that morphological changes and a one-handed helical structure of poly(phenylacetylene)s can be observed on a solid substrate using AFM. Therefore, AFM may be applicable as a novel analytical tool for directly detecting the macromolecular helicity of optically active polymers. We have prepared a number of helical polymers bearing various functional groups,[8−10] and their chiroptical properties on a solid substrate can be investigated using AFM. We believe that the AFM technique combined with helical polymers induced by chiral molecules is expected to offer a specific sensory system for the direct detection of the chirality of small chiral molecules and biomolecules.

Acknowledgment. This work was partially supported by a Grant-in-Aid for Scientific Research from the Japan Society for the Promotion of Science and the Ministry of Education, Culture, Sports, Science, and Technology, Japan.

Supporting Information Available: Experimental procedures, AFM images of poly-**1H** with and without (*R*)-Nap on HOPG, histograms of the height distribution of poly-**1H**, the poly-**1H**−(*R*)-Nap complex, and poly-(*R*)-**2**, CD spectra of poly-**1H** with (*R*)-Nap and poly-(*R*)-**2** in DMSO and DMF, respectively, characteristics of poly-**1L**, poly-**1H**, and poly-(*R*)-**2**, and expanded AFM phase images of the poly-**1H**−(*R*)-Nap complex and poly-(*R*)-**2** (PDF). This material is available free of charge via the Internet at http://pubs.acs.org.

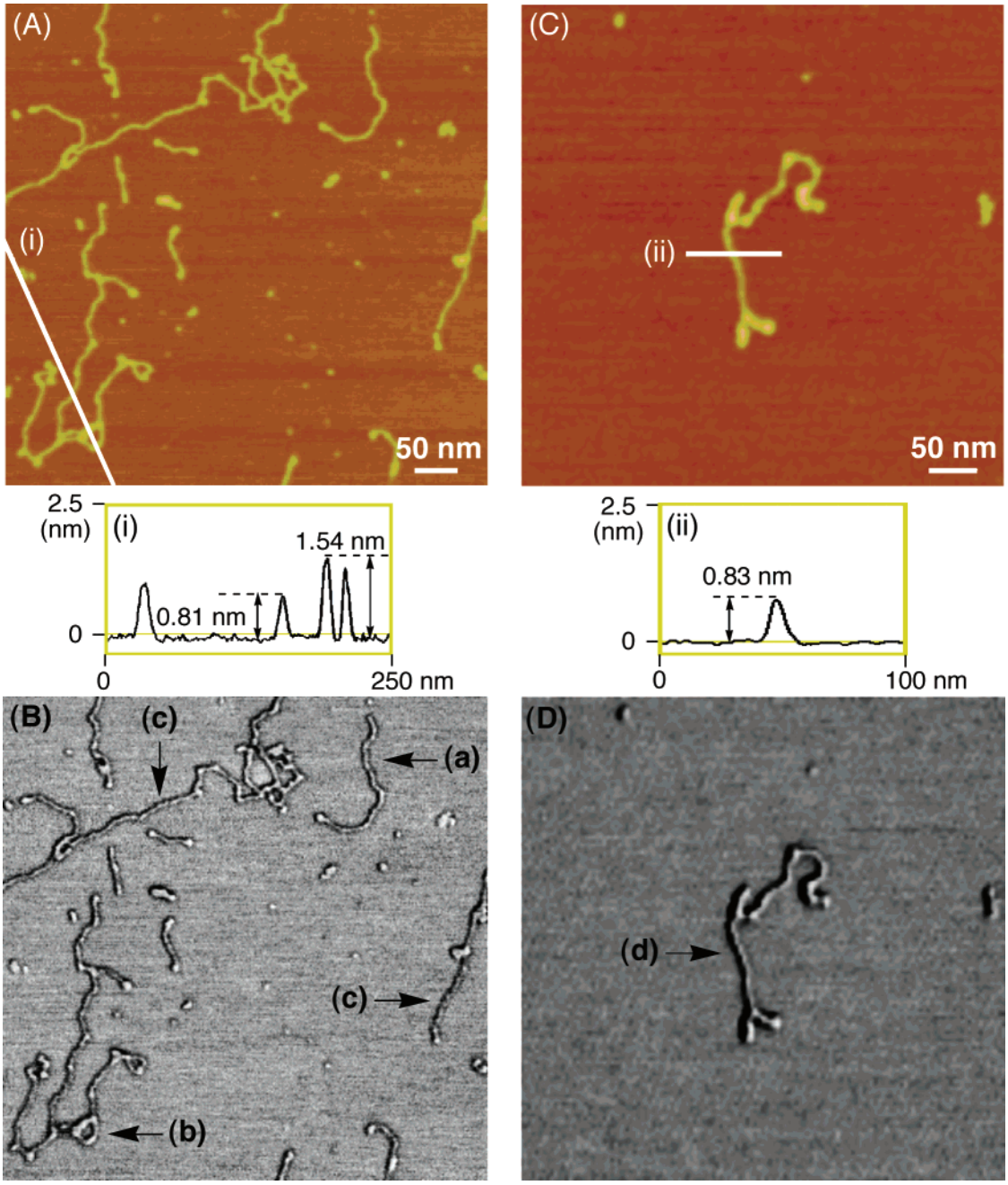

Figure 4. Expanded AFM height (A and C) and phase (B and D) images of the poly-**1H**−(*R*)-Nap complex (A and B) and poly-(*R*)-**2** on mica (C and D). These images are from Figures 2D and 3, respectively. A single molecule (a), a toroidal structure (b), and helical structures (c) can be seen in part B. A helical structure is also visualized in the phase image (D). Cross section profiles in parts A (i) and C (ii) are shown (middle).

References and Notes

(1) (a) Hansma, H. G.; Vesenka, J.; Siegerist, C.; Kelderman, G.; Morrett, H.; Sinsheimer, R. L.; Elings, V.; Bustamante, C.; Hansma, P. K. *Science* **1992**, *256*, 1180−1184. (b) Ionescu-Zanetti, C.; Khurana, R.; Gillespie, J. R.; Petrick, J. S.; Trabachino, L. C.; Minert, L. J.; Carter, S. A.; Fink, A. L. *Proc. Natl. Acad. Sci. U.S.A.* **1999**, *96*, 13175−13179. (c) Maeda, Y.; Matsumoto, T.; Tanaka, H.; Kawai, T. *Jpn. J. Appl. Phys.* **1999**, *38*, L1211−L1212.

(2) (a) Kumaki, J.; Nishikawa, Y.; Hashimoto, T. *J. Am. Chem. Soc.* **1996**, *118*, 3321−3322. (b) Percec, V.; Ahn, C.-H.; Ungar, G.; Yeardley, D. J. P.; Möller, M.; Sheiko, S. S. *Nature* **1998**, *391*, 161−164. (c) Börner, H. G.; Duran, D.; Matyjaszewski, K.; da Silva, M.; Sheiko, S. S. *Macromolecules* **2002**, *35*, 3387−3394. (d) Kumaki, J.; Hashimoto, T. *J. Am. Chem. Soc.* **2003**, *125*, 4907−4917.

(3) Sheiko, S. S.; Möller, M. *Chem. Rev.* **2001**, *101*, 4099−4123.

(4) Minko, S.; Kiriy, A.; Gorodyska, G.; Stamm, M. *J. Am. Chem. Soc.* **2002**, *124*, 3218−3219.

(5) (a) Nyffenegger, R. M.; Penner, R. M. *Chem. Rev.* **1997**, *97*, 1195−1230. (b) Piner, R. D.; Zhu, J.; Xu, F.; Hong, S.; Mirkin, C. A. *Science* **1999**, *283*, 661−663.

(6) (a) Furukawa, K.; Ebata, K.; Fujiki, M. *Adv. Mater.* **2000**, *12*, 1033−1036. (b) Cornelissen, J. J. L. M.; Donners, J. J. J. M.; de Gelder, R.; Graswinckel, W. S.; Metselaar, G. A.; Rowan, A. E.; Sommerdijk, N. A. J. M.; Nolte, R. J. M. *Science* **2001**, *293*, 676−680. (c) Li, B. S.; Cheuk, K. K. L.; Salhi, F.; Lam, J. W. Y.; Cha, J. A. K.; Xiao, X.; Bai, C.; Tang, B. Z. *Nano Lett.* **2001**, *1*, 323−328. (d) Nishimura, T.; Takatani, K.; Sakurai, S.; Maeda, K.; Yashima, E. *Angew. Chem., Int. Ed.* **2002**, *41*, 3602−3604. (e) Li, B. S.; Cheuk, K. K. L.; Ling, L.; Chen, J.; Xiao, X.; Bai, C.; Tang, B. Z. *Macromolecules* **2003**, *36*, 77−85. (f) Imase, T.; Ohira, A.; Okoshi, K.; Sano, N.; Kawauchi, S.; Watanabe, J.; Kunitake, M. *Macromolecules* **2003**, *36*, 1865−1869. (g) Kiriy, N.; Jähne, E.; Adler, H.-J.; Schneider, M.; Kiriy, A.; Gorodyska, G.; Minko, S.; Jehnichen, D.; Simon, P.; Fokin, A. A.; Stamm, M. *Nano Lett.* **2003**, *3*, 707−712. (h) Li, B.

S.; Cheuk, K. K. L.; Yang, D.; Lam, J. W. Y.; Wan, L. J.; Bai, C.; Tang, B. Z. *Macromolecules* **2003**, *36*, 5447−5450.
(7) Shinohara, K.; Yasuda, S.; Kato, G.; Fujita, M.; Shigekawa, H. *J. Am. Chem. Soc.* **2001**, *123*, 3619−3620.
(8) (a) Yashima, E.; Matsushima, T.; Okamoto, Y. *J. Am. Chem. Soc.* **1995**, *117*, 11596−11597. (b) Yashima, E.; Maeda, Y.; Okamoto, Y. *Chem. Lett.* **1996**, 955−956. (c) Yashima, E.; Matsushima, T.; Okamoto, Y. *J. Am. Chem. Soc.* **1997**, *119*, 6345−6359. (d) Yashima, E.; Maeda, K.; Okamoto, Y. *Nature* **1999**, *399*, 449−451. (e) Nonokawa, R.; Yashima, E. *J. Am. Chem. Soc.* **2003**, *125*, 1278−1283.
(9) (a) Yashima, E.; Nimura, T.; Matsushima, T.; Okamoto, Y. *J. Am. Chem. Soc.* **1996**, *118*, 9800−9801. (b) Saito, M. A.; Maeda, K.; Onouchi, H.; Yashima, E. *Macromolecules* **2000**, *33*, 4616−4618. (c) Onouchi, H.; Maeda, K.; Yashima, E. *J. Am. Chem. Soc.* **2001**, *123*, 7441−7442. (d) Maeda, K.; Goto, H.; Yashima, E. *Macromolecules* **2001**, *34*, 1160−1164.
(10) (a) Yashima, E.; Huang, S.; Matsushima, T.; Okamoto, Y. *Macromolecules* **1995**, *28*, 4184−4193. (b) Morino, K.; Maeda, K.; Okamoto, Y.; Yashima, E.; Sato, T. *Chem.—Eur. J.* **2002**, *8*, 5112−5120. (c) Morino, K.; Maeda, K.; Yashima, E. *Macromolecules* **2003**, *36*, 1480−1486.
(11) On the other hand, the AFM images on HOPG prepared with the same procedure as that on mica revealed micrometer-scaled, aggregated polymer strands and clusters because of the repulsive interactions between the hydrophilic poly-**1H** and poly-**1H**−(*R*)-Nap and the hydrophobic HOPG surface (Supporting Information). See ref 6d and: Das, G.; Ouali, L.; Adrian, M.; Baumeister, B.; Wilkinson, K. J.; Matile, S. *Angew. Chem., Int. Ed.* **2001**, *40*, 4657−4661.
(12) (a) Prokhorova, S. A.; Sheiko, S. S.; Möller, M.; Ahn, C.-H.; Percec, V. *Macromol. Rapid Commun.* **1998**, *19*, 359−366. (b) Uchihashi, T.; Choi, N.; Tanigawa, M.; Ashino, M.; Sugawara, Y.; Nishijima, H.; Akita, S.; Nakayama, Y.; Tokumoto, H.; Yokoyama, K.; Morita, S.; Ishikawa, M. *Jpn. J. Appl. Phys.* **2000**, *39*, L887−L889. (c) Gao, S.; Chi, L.; Lenhert, S.; Anczykowski, B.; Niemeyer, C. M.; Adler, M.; Fuchs, H. *ChemPhysChem* **2001**, *6*, 384−388.
(13) (a) Leclére, P.; Calderone, A.; Marsitzky, D.; Francke, V.; Geerts, Y.; Müllen, K.; Brédas, J. L.; Lazzaroni, R. *Adv. Mater.* **2000**, *12*, 1042−1046. (b) Lashuel, H. A.; LaBrenz, S. R.; Woo, L.; Serpell, L. C.; Kelly, J. W. *J. Am. Chem. Soc.* **2000**, *122*, 5262−5277.
(14) Under a relatively high poly-(*R*)-**2** concentration (more than 0.05 mg/mL), poly-(*R*)-**2** intermolecularly aggregates on the basis of the height analysis, whereas individual poly-(*R*)-**2** molecules can be visualized on mica prepared from a dilute solution of poly-(*R*)-**2** (0.025 mg/mL).
(15) We attempted to determine the average molecular lengths of poly-**1H** (calculated length as 203 nm based on its M_n and computer simulation (Figure 1B)) and poly-**1H** complexed with (*R*)-Nap, but it was impossible because we unexpectedly observed long polymer chains (Figure 2C and D) probably through a partial interchain interaction or the "sticky end" biting. See: (a) Mao, C.; LaBean, T. H.; Reif, J. H.; Seeman, N. C. *Nature* **2000**, *407*, 493−496. (b) Pandya, M. J.; Spooner, G. M.; Sunde, M.; Thorpe, J. R.; Rodger, A.; Woolfson, D. N. *Biochemistry* **2000**, *39*, 8728−8734.

MA035290T